Macromolecules

Article

pubs.acs.org/Macromolecules

Polyelectrolyte Composite: Hyaluronic Acid Mixture with DNA

Ida Delač Marion,[†] Danijel Grgičin,[†] Krešimir Salamon,[†] Sigrid Bernstorff,[‡] and Tomislav Vuletić*[,†]

[†]Institut za fiziku, Bijenička 46, 10000 Zagreb, Croatia

[‡]Elettra-Sincrotrone Trieste, 34149 Basovizza, Italy

Supporting Information

ABSTRACT: We studied salt-free, highly concentrated (5−200 g/L) mixtures of unfragmented (μm contour length) DNA and hyaluronic acid (HA) as a borderline example of rigid-rod/flexible-chain composite, across a broad range of concentration ratios c_{HA}/c_{DNA} = 0.05−50. By polarizing microscopy, we established that the DNA and HA form clearly separated thread-like domains defined and oriented by solution shear. Within its domains, DNA shows birefringent banded patterns, routinely observed for long chain mesogens. We applied small-angle X-ray scattering (SAXS) to the mixtures and observed a polyelectrolyte (PE) correlation peak at $q^\star$ wave vector. This peak was ascribed to DNA subphase and was used as a measure of the effective DNA concentration in the subphase $c^\star_{DNA}$, according to deGennes scaling relationship between the DNA mesh size $\xi = 2\pi/q^\star \propto c^{-1/2}$ and monomer concentration c. From $c^\star_{DNA}$ (and initial c_{HA} and c_{DNA}), we inferred the effective $c^\star_{HA}$ of HA subphase. We find a concentration-independent ratio $\Gamma = c^\star_{HA}/c^\star_{DNA} \approx 0.85$ across a broad range of 0.02−0.4 M. As there is the osmotic pressure (Π) equilibrium between DNA and HA subphases, the constant Γ indicates that $\Pi \propto c^{9/8}$ scaling common for DNA and other highly charged PEs is valid also for HA (a weak PE—does not feature counterion condensation). Therefore, we propose that this deviation from the conventional osmotic pressure scaling $\Pi \propto c$ cannot originate from the concentration dependence of counterion condensation, which is an implicit but common interpretation in the literature. Further, as HA releases all its counterions into the solution, the HA osmotic coefficient ϕ_{HA} we took as a measure of the DNA osmotic coefficient which we found to be $\phi_{DNA} \approx 0.28$. This, double the Manning value, corroborates a result by Raspaud et al.[1]

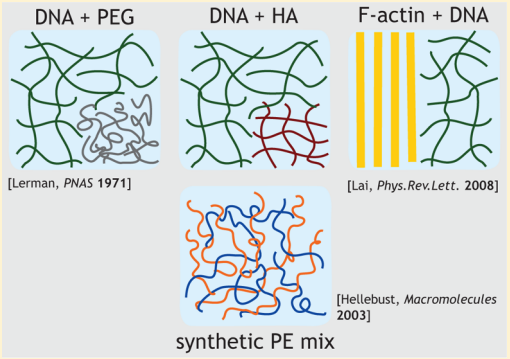

INTRODUCTION

Most biomacromolecules are polyelectrolytes (PEs)—polymers with ionizable groups on constituent monomers. PEs dissociate in polar solvents (water being the natural one) into polyions and a cloud of oppositely charged, low-molecular weight counterions. The long-range electrostatic interaction of these charged species leads to a spatial arrangement and dynamics qualitatively different than for neutral polymers. The arrangement (polyion conformation and counterion distribution) depends on their concentration but also on the polyion size, valence of counterions, and especially the added salt concentration and valence.[2−5] The polyion subsystem is different from a neutral polymer due to the electrostatic contribution L_e to the structural (intrinsic) persistence length L_0 (a measure of the polyion chain rigidity). The former is dependent on the screening of the charges on the chain by all the ions in the cloud (counterions and added-salt ions). The electrostatic contribution may easily surpass the structural one in low added salt conditions.[6−10]

For the counterions, it is entropically favorable to disperse away from the polyion, while the electrostatics tend to keep them in the vicinity. The distribution of counterions was already very early studied for a single, infinite rodlike polyion, within a mean-field Poisson−Boltzmann theory.[11] The strong electrical field originating from the polyion renders PEs much less tractable than electrolytes, where the Debye−Hückel (DH) approximation works well. The issue was simplified within the two-state model developed by Manning and Oosawa[12,13]—they assumed that counterions are to be divided into those that are free, away from the polyion potential (where even the DH approximation may be valid), and those that remain very close to the polyion, condensed within some finite distance, thus reducing the polyion charge. Condensation occurs only for polyions of higher linear charge $\eta = l_B/b > 1$, where l_B is the Bjerrum length and b is the distance between the charges along the polyion—condensation reduces the polyion charge density down to $\eta = 1$. This counterion condensation phenomenon, along with the above electrostatic persistence length, continues to be of primary importance in understanding PEs.[5,14−18]

One experimentally accessible parameter where both the polyions and counterions come into play is the osmotic pressure.[5] In the low added salt limit, the osmotic pressure of PEs could be proportional to the pressure from the ideal gas of counterions of concentration c, $\Pi_{ion}/RT = c$. Any deviation from this is accounted for with the osmotic pressure coefficient $\phi < 1$. Notably, within the Manning model $\phi = (2\eta)^{-1}$ for

Received: October 11, 2014
Revised: February 4, 2015

DOI: 10.1021/ma502090x
Macromolecules XXXX, XXX, XXX−XXX

strong PEs with $\eta > 1$, while $\phi = 1-(1/2)\eta$ for weak PEs with $\eta < 1$.[13]

Polyions could also contribute to the osmotic pressure of PE. One way to describe a polyion is to take it as composed of rigid segments (Kuhn lengths). These are comparable to the persistence length, L_p. This picture is more applicable to dilute solutions. At higher concentrations, in the semidilute regime, the relevant length scale is the correlation volume size (length) ξ. The respective contribution to the osmotic pressure is $\Pi_{chain}/RT = \xi^{-3}$. Inevitably, the polyion contribution will be negligible up to at least 0.5−1 M (monomolar) concentrations where the correlation length is reduced down to a few nm.[19] In order to take the polyions into account and describe the osmotic pressure of PEs, one may start from the scaling arguments for uncharged polymers first. This approach was well summarized by Wang and Bloomfield.[20] The uncharged polymer size is the Flory radius which scales as $R_F \propto N^{3/5}$ (N = polymerization degree). The overlap concentration of separate chains scales as $c^\star \approx N/R_F^3$. The osmotic pressure Π of a semidilute system should not depend on N—the separate chains lose their identity in the semidilute regime. Thus, Π should be a function of only the monomer concentration: $\Pi = F(c/c^\star)$. Combining these expressions we get that $\Pi \propto (c/c^\star)^{9/4}$, which has been extensively confirmed experimentally.[20] Now, charged polymer (PE) in a high added salt environment should behave in a similar manner, as the screening reduces the interchain interactions. However, effects of charge interactions along the chain should be taken into account. A measure for the interaction along the chain is the electrostatic persistence length L_e, which should be compared to the Debye screening length $\kappa^{-1} \propto c^{-1/2}$ that scales with the square-root of the ionic concentration. Odijk[8] gave the osmotic pressure for a semidilute salt-free PE with $\Pi \propto (L_e/\kappa)^{3/4}c^{9/4}$. Both L_e and κ^{-1} are defined by the counterion (i.e. monomer) concentration. The above expression then reduces to

$$\Pi \propto c^{9/8} \tag{1}$$

This scaling has been well substantiated for strong PEs, DNA ($\xi = 4.2$) and polystyrene-sulfonate, PSS ($\xi = 2.9$)[1,20−22] with the osmotic equilibration method. Deviation from 9/8 scaling to 9/4 scaling, the latter being a characteristic of uncharged polymers, was indeed found around 0.5 M (monomolar) concentrations. There the osmotic pressure becomes dominated by conventional, uncharged polymer depletion effects.

Indicatively, Essaffi et al.[23] mention, in their study of synthetic PEs, the issue of deviation from $\Pi \propto c$ scaling to be due to the polyion contribution and therefore proceed to analyze their results only below about 0.2 M where they consider it to be negligible compared to the counterion contribution. However, the region below 0.2 M is also the region where the above-mentioned 9/8 scaling applies—the scaling that deviates from $\Pi \propto c$ due to polyion contribution. Nevertheless, Essaffi et al. interpreted their results by taking the exponent of 1 to be appropriate and any deviation from this law is eventually included in the osmotic coefficient (i.e.counterion condensation) dependence on concentration. This view is quite general.[22,24−27] In other words, it is debatable whether the deviation from $\Pi \propto c$ scaling observed in PEs is due to $\Pi \propto \phi(c)\cdot c$ or due to $\Pi \propto c^{9/8}$.[28]

Interestingly, weak PEs have not been studied with the intent of comparison with strong PE in mind. Do they feature deviation from $\Pi \propto c$ while lacking condensation and its presumed concentration dependent effects on the osmotic pressure? This would indicate in what manner to take into account the polyion chains contribution. Theories and simulations to get $\Pi \propto \phi(c)\cdot c$ apparently always deal with strong PEs, focusing on the condensation phenomenon, assuming that $\phi(c)$ can only be due to condensation, not polyions. One of the reasons is that synthetic PEs, where one may reduce the chemical charge and thus prepare a weak linear charge PE, concomitantly with becoming weakly charged also lose solubility in water.[23] In other words, a system of interest in studies of PEs, for the reasons of comparison, have also to be weak PEs. A common experimental system for osmotic pressure studies is PE brought in contact with a neutral polymer—osmotic stressing agent (e.g., PEG - polyethylene glycol)—for which the osmotic pressure versus concentration dependence has been separately measured.[29−34] This contact does not necessitate a semipermeable membrane, as the high molecular weight of the components suppresses the mixing. That is, the translational entropy loss due to the phase separation is N times smaller (N = number of links in the chain) than for small molecules of similar volume fraction, while the energy gain from the contact of links is the same. This occurs even if there is no interaction (Flory parameter $\chi = 0$) between those links.[35]

We consider that we may provide more insightful and conclusive results by investigating a mixture of a strong and a weak poylelectrolyte, thus directly comparing their osmotic pressure behavior. Therefore, we present here a study of DNA and hyaluronic acid (HA) mixture with nominal DNA and/or HA concentrations covering the range of 5−100 g/L. A polysaccharide, HA is a weak PE with one charge per monomer of the length $b_H = 1\ nm$, so $\eta_H = l_B/b = 0.7 < 1$,[36] and its counterions should remain free. HA is a prominent component in the extracellular matrix,[37−40] and the PE properties render it relevant in a multitude roles in living matter.

For HA, the osmotic pressure behavior in very low added salt environment is lacking,[41−48] and we may arrive at this by producing a comparison with the well studied DNA. That is, our aim was to compare the osmotical pressures and/or uncondensed counterion concentrations of a strong and a weak PE in a mixture. Indeed, our principal result is that for HA, as well as for DNA (or another strong PE, PSS), the scaling[20,22] $\Pi \propto c^{9/8}$ is valid up to 400−500 mM (monomers). To this conclusion, we arrive from our finding that the monomer concentrations of DNA and HA in the mixture are in a constant ratio across the concentration range (20−400 mM) studied, which is only possible if they obey the same scaling. Finally, because with HA there is no condensation, we take the osmotic coeficient of HA to serve as a reference for the DNA coefficient.

With this study of HA and DNA PE composite, we managed to address also some other issues:

- HA is a semiflexible PE ($L_0 \approx 10$ nm) more akin to DNA ($L_0 = 50$ nm) than the synthetic PEs. The above osmotic pressure study requests that HA and DNA do not mix and we do confirm this. An example of a completely phase-separating like-charged PEs mixture is the DNA mixture with rodlike PE, F-actin ($L_0 = 10\ \mu$m). F-actin forms separate, nematic phases when mixed with DNA in pure water/low salt.[49] Interestingly, the DNA, as the flexible component, has a functional role of the osmotic stressing agent. Intuitively, the demixing tendencies should be stronger in the case of the repulsive Coulomb interactions between two similarly charged polyionic

DOI: 10.1021/ma502090x
Macromolecules XXXX, XXX, XXX−XXX

chains in a mixture. However, here we should not forget that the Coulomb repulsion is there also for the chains of the same type, competing with the previous interaction. Studies of synthetic, flexible PEs have shown demixing above 5−15% PE content in aqueous solution, but in a non-negligible region of the phase diagram complete mixing does occur.[50,51]

- HA does not feature the PE correlation peak in the small-angle X-ray scattering (SAXS) intensity. This peak is the signature of strong electrostatic interactions among polyions of PEs of higher linear charge.[43,48] We base this also on our recent SAXS study of DNA and HA solutions in very low added salt.[52] What we found here is that, as in the case of F-actin/DNA mixture, only the more rigid and more strongly charged PE defines the scattering signal. In other words, here, in SAXS we only detect DNA domains via their PE scattering peaks, the position of which scales nicely with DNA concentration - in other words, with SAXS we precisely measured the effective concentrations of DNA in the respective subphase.

EXPERIMENTAL SECTION

Materials. Solutions and mixtures of deoxyribonucleic acid (DNA) and hyaluronic acid (HA) solutions, both in the form of sodium salts, were prepared with ultrapure water (Millipore Milli-Q), without addition of any simple salts. Dissolving without a buffer leads to a solution where the pH is defined by the CO_2 dissolved in water, which leads to a pH of about 6, with both DNA ($pK_a = 0$) and HA ($pK_a = 3.2$[46]) fully ionized. In our previous studies,[52−56] we used the DNA and HA samples described below, and we ascertained that the salt content in these samples is negligible, less than one added salt ion per 10 monomers. As such, samples dissolved in ultrapure water are taken to be free of added salt.

For DNA samples we used Salmon testes lyophilized DNA obtained from Sigma-Aldrich (cat. no. D1626) which is polydisperse, with chain lengths in the range from 2 kbp to 20 kbp or higher (contour length 0.7−7 μm). For HA we used HA from Streptococcus equi sp. from Sigma-Aldrich (cat. no. Fluka53747) with an average polymerization degree of 4000 (contour length of 4 μm) and a polydispersity index 1.3. For both, the low protein content is declared by the manufacturer. Because they have rather long chain lengths, the corresponding dilute−semidilute crossover concentrations are expected to be several orders of magnitude below the concentration range studied[57,58] so we conclude that our samples are in the semidilute regime.

We had two sets of samples prepared according to the following protocols (concentrations are given as dry mass per total volume of the sample):

Protocol I - for SAXS and polarizing microscopy (PM). We prepared mother solutions of DNA with concentrations 5−80 g/L by adding a given amount of dry DNA fibers (5−80 mg) and ultrapure water (1 mL) into a small polyethylene bag each. During the course of the experiment, more and more dry HA grains were being added to these bags, thus resulting in an increasing HA concentration in the binary DNA/HA mixture, at a fixed DNA concentration. The maximum HA added was about 100 mg per 1 mL DNA solution (10% by volume) and dissolving HA could not have swollen the total volume more than a couple of percent beyond 1 mL. For the purpose of our analysis, the consequent deviation in DNA concentration is negligible. The range of both polyelectrolyte concentrations is shown in Figure 1. The preparation procedure for each consecutive HA concentration was the following: first, a small cut was made in a bag with the mother solution and a couple of μL of sample was extracted from the plastic bag (in a manner toothpaste is squeezed out) and onto either the SAXS sample holder or onto a glass slide for PM. The bag was weighed to establish the amount of sample extracted. Although the measurement was conducted on the previous sample, dry HA was added to the bag with the solution, the bag was sealed (welded) and weighed as a control of the added mass. The bag was then squished between fingers for several minutes to ensure complete dissolution of HA and thorough mixing of the contents. A next sample (now with the next higher HA concentration) was then extracted and applied in the same manner like the previous one thus completing the cycle. This was done up to about 100 g/L of HA, for each of the DNA solutions.

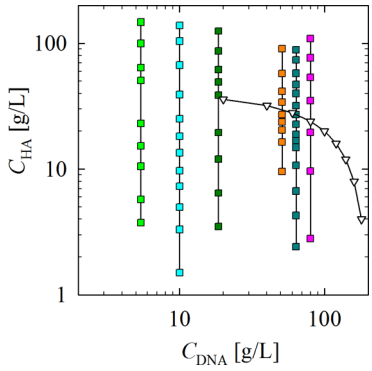

Figure 1. Mass concentrations of DNA and HA in the binary mixtures prepared by Protocol I (squares) and Protocol II (triangles). Vertical lines denote different DNA mother solutions that have been gradually complemented with HA.

Protocol II - for SAXS. We prepared mother solutions of both DNA (C_{DNA} = 200 g/L) and HA (C_{HA} = 40 g/L). These were then mixed in 10% steps (90:10, 80:20, ..., 10:90) which resulted in 9 (+2 mother solutions) different solutions across the range from pure DNA to pure HA. We emphasize that, unlike the protocol I where HA grains were mixed into the solution, here we mixed two solutions which were allowed to equilibrate for a month. Nevertheless, no qualitative or quantitative difference in properties was observed for these samples when compared to protocol I (see later Figure 7). The DNA mother solution C_{DNA} from this set was also used for establishing the dependence of the polyelectrolyte correlation peak observed in SAXS versus DNA concentration (see Supporting Information).

METHODS

Small-Angle X-ray Scattering. The SAXS measurements have been carried out at the high-flux SAXS beamline at the ELETTRA synchrotron light source (Trieste, Italy).[59] The scattering patterns were recorded with a 2D image plate detector (Mar300, MarResearch, Norderstedt, Germany) positioned at the distance L = 1.32 m from the sample. The detector covered the q-range ($q = 4\pi (\sin\theta)/\lambda$, where λ = 1.54 Å is the wavelength and 2θ is the scattering angle) of interest from q_{min} = 0.16 nm^{-1} to q_{max} = 5.9 nm^{-1}. The angular calibration of the detector was performed with silver behenate powder (d-spacing of 58.4 Å). The X-ray beam size at the sample position was set to 0.5 × 3.0 mm^2 ($V \times H$).

The sample solutions were measured either in quartz glass capillaries with a diameter of 1 mm or in a specially designed gel-sample-holder, enclosed between two layers of mylar, depending on the sample solution viscosity. The measurements were performed at 25 °C.

Care was taken that no radiation damage was affecting the samples. This was done by recording multiple short frames (10 s each) on the same sample volume of several DNA (20, 40, and 60 g/L), HA (10, 20, and 30 g/L) and some binary DNA/HA mixtures, thereby ascertaining the maximum acquisition time during which no change of the scattering pattern occurred. For all solutions which contain DNA, a decrease of scattered intensity was observed after the 8th frame, while for pure HA solutions the scattering intensity was persistent even after the 60th frame. This finding indicates that some DNA chain degradation occurs, likely induced by the high flux of the beam. Thus, we selected 60 s as an exposure time for measuring the radiation scattered by the samples.

DOI: 10.1021/ma502090x
Macromolecules XXXX, XXX, XXX−XXX

Before the analysis, the 2D-images were corrected for the detector response and the background scattering (pure H_20) was subtracted. From each 2D-image, 1D scattering profiles (curves) at several azimuths were extracted in order to quantitatively analyze the scattering intensities for each DNA/HA mixture.

Polarization Microscopy. Polarizing microscopy (PLM) observations were done between a slide and coverslip. To prevent dehydration, the preparations were sealed by epoxy. The thickness of the preparations was ranging from 50 to 200 μm. We used an Optika N-400 POL polarizing microscope with Optikam B5 digital camera. A quartz first order retardation plate (λ-plate) was inserted at 45° between crossed polars to analyze the orientations of molecules in particular domains.

RESULTS

Phase Separation. Polarizing microscopy offers an immediate insight in the nature of the mixture of DNA and HA. That is, we remind that well-defined mesophases are routinely formed with fragmented, monodisperse DNA, s.c. nucleosomal DNA. These fragments are around 50 nm or 150 bp and feature cholesteric patterns above 100−150 g/L and columnar hexagonal above 300 g/L.[60] Long (in μm), unfragmented DNA strands in solution may align in parallel and present birefringent textures in polarizing microscopy. Long DNA does not reach liquid crystalline phases like fragmented DNA, but the ordering starts at quite lower concetrations, below 20 g/L.[61,62] On the other hand, HA is not known to show supramolecular organization that could be detected due to its birefringence. A principal birefringent texture for long polymers are banded patterns, which form for DNA but also for other polymers, e.g., xanthan (a polysaccharide but a helical, chiral molecule) (see ref 63 and refs therein). In DNA solutions, these patterns occur without a defined boundary between isotropic and birefringent regions of the sample. This is unlike, e.g., cholesteric droplets, formed by shorter mesogenic molecules, which are well-defined against isotropic background.

Our PLM images of DNA/HA mixtures consistently show coexistence of nonbirefringent and birefringent domains. In Figure 2, we show PLM images from a mixture of 49 g/L DNA and 18 g/L HA that have been left to equilibrate for 6 months (sealed between a slide and a coverslip). Images are taken with a λ plate (full wave retardation plate) inserted in the optical path between the crossed polars, after the sample. This allows determination of the orientation of macromolecules. Dashed lines in the images denote the general orientation of macromolecules in a large rope-like domain that contains many aligned strands. When the rope is parallel to the fast axis of the λ-plate (Figure 2a), it is colored yellow/orange (as negatively birefringent DNA should be), and when perpendicular (90° rotated sample, Figure 2c), the rope turns blue. At 45° (mid panel, Figure 2b), it is almost extinguished. Optically isotropic (nonbirefringent) domains are consistenly red/magenta tinted independent of the sample rotation. The appearance of the mixture is directly reminiscent of unfragmented DNA mixture with neutral, flexible polymer like polyethylene glycol (PEG);[60] in the mixture, DNA and PEG remain in separated domains. PEG is routinely used to induce DNA condensation and mesophase formation, and here, presumably HA takes this role. This is our first indication that the isotropic domains do not contain DNA but only HA. Even if isotropic, HA domains did contain some DNA, its concentration must be below 10 g/L, otherwise the domains would show some birefringence.

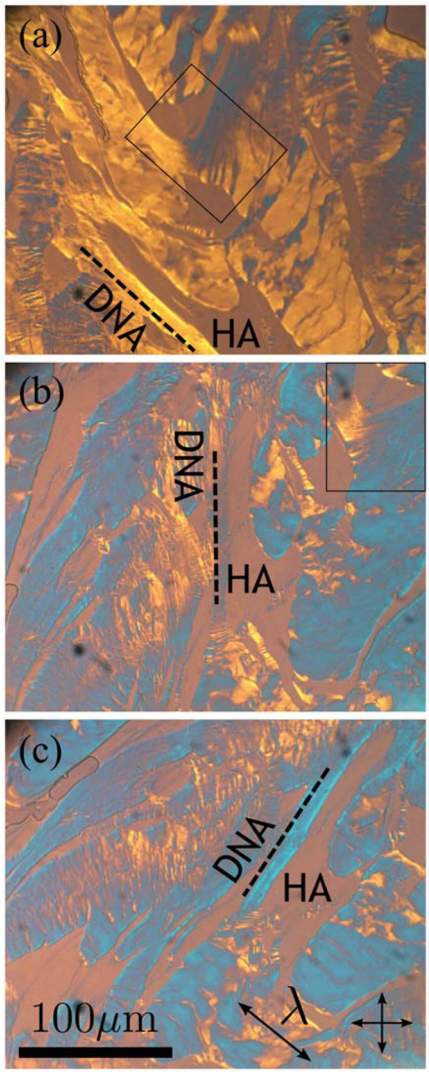

Figure 2. Polarizing microscopy (PLM) images taken with λ-plate inserted, of DNA 49 g/L + 18 g/L HA mixtures. Birefringent, presumably DNA domains are orange or blue, while nonbirefringent, presumably HA domains are red. Dashed lines denote the orientation of negatively birefringent DNA molecules, highly aligned in a rope. The rope appears (a) orange when the chains are parallel to the λ-plate fast axis (λ-arrow), (b) blue when perpendicular, and (c) extinguish when at 45°. Crossed arrows denote the orientation of the crossed polars. Rectangles denote the area enlarged in Figure 3.

In Figure 3, the banded pattern region from Figure 2a (rectangle) is enlarged. Banded patterns are distinct from apparently similar cholesteric textures in the manner that the relative thickness of the bands (of different coloring) changes upon rotation of the sample. Between Figure 2a,c, blue or yellow bands dominate for different orientations. In the present preparation, the banded pattern is formed at the end of the highly aligned rope when the molecules from the rope fan out and expand between two isotropic domains. On the right-hand side, the strands are undulating, change local orientation periodically, which leads to appearance of the bands, as denoted by the schematics in the image. On the left-hand side, the strands are extended along the neighboring isotropic domain and no bands are visible.

Solution Anisotropy. Figure 4 shows a series of 2D SAXS patterns for DNA/HA samples at various additions of HA and

DOI: 10.1021/ma502090x
Macromolecules XXXX, XXX, XXX−XXX

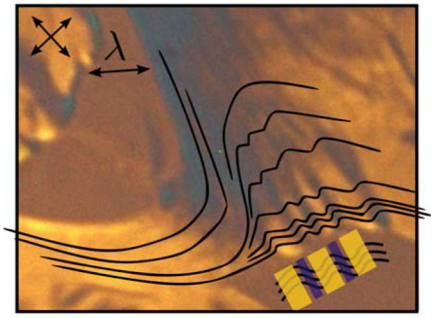

Figure 3. Enlarged area from Figure 2a presents banded patterns typical of long polymers. Upon 45° rotation, the local orientation of the undulating DNA strands in relation to the λ-plate axis (λ-arrow) changes as does the coloring of the bands. Lines represent the orientation of DNA molecules. Crossed arrows denote the orientation of the crossed polars.

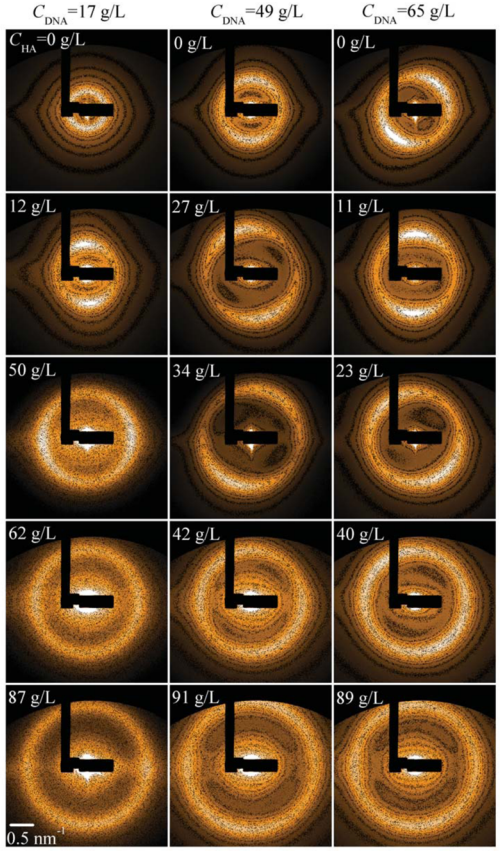

Figure 4. Selected 2D-SAXS patterns for three different fixed nominal DNA concentrations (for each column) and with different amount of HA added (in rows).

grouped by DNA mass concentration, C_{DNA}: 17 g/L, 49 g/L, and 65 g/L in the first, second, and third column, respectively. The main feature observed for all of the measured DNA/HA binary solutions is the appearance of the ring-like scattering maximum, indicating the existence of a short-range ordered structure in the solutions. As PE chains are negatively charged, the repulsive interaction between them produces a short-range ordered mesh which is revealed in SAXS experiments through a more or less intense scattering maximum at $q^{\star}$. We know from our recent work[52] (as well from other works[44,48]) that the pure HA solutions show only a relatively weak and wide shoulder in scattering intensities, unlike the DNA solutions. The reason is that the sugar groups located on the HA chain lack the scattering power of relatively heavy P atoms present in the phosphate groups of a DNA chain. DNA also retains in its vicinity relatively heavier Na^+ counterions,[17] unlike HA (which features no Manning condensation). The absence of a clear scattering maximum is also a consequence of the more disordered mesh due to the weaker electrostatic interaction between HA chains that are of lower linear charge density. Thus, for DNA/HA binary mixtures, the signal should be dominated by the DNA macroion partial scattering function. Taking into account the lack of a clear maximum for pure HA solutions, we can conclude that the appearance of the scattering maximum in the SAXS spectra for DNA/HA solutions visible in Figure 4 has its origin only in the DNA interchain arrangement.

For DNA sample C_{DNA} = 17 g/L without HA addition (first column, first row in Figure 4), the SAXS ring is isotropic in intensity distribution. By adding HA in this DNA mother solution (down the columns in Figure 4), as well as with the increase of DNA concentration for HA free samples (along the first row in Figure 4), one may notice that the azimuthal intensity distribution at the peak position of the ring becomes anisotropic. The anisotropy in scattering has 2-fold symmetry which indicates a preferential orientation of the DNA macroions, at least across the scattering volume (0.5 × 0.5 × 3 mm). Moreover, the appearance of anisotropy in SAXS correlates with the appearance of birefringence due to the alignment of DNA strands in the sample. For example, C_{DNA} = 17 g/L DNA without HA is nonbirefringent in PLM and isotropic in SAXS, while C_{DNA} = 17 g/L DNA with C_{HA} = 12 g/L HA shows a weak birefringence that occurs across a large portion of the preparation between the slide and coverslip and is anisotropic in SAXS (second row, first image in Figure 4) One may check also the Supporting Information for comparison of PLM images of C_{DNA} = 40 g/L DNA with HA contents C_{HA} = 18 g/L, 42 g/L, and 87 g/L with the respective SAXS patterns presented in Figure 4 (central column). Our DNA/HA mixture shows (see Figure 2) isolated and rope-like birefringent domains formed from aligned DNA strands. A typical length of these domains is of the order of 100 μm. This means that the scattering volume contains of the order of 10^2–10^3 domains which should be, in principle, randomly oriented and produce isotropic SAXS patterns. However, we believe that DNA domains acquire a preferential direction during insertion of DNA/HA mixture into the SAXS sample holder. Namely, as most of the DNA/HA mixtures are viscous, they were inserted into SAXS sample holder by squeezing them out from the small hole made on the corner of plastic bag wherein they have been prepared and mixed. Thus, the sample was under shear and flow and the domains reoriented themselves along,[48,64] eventually producing the anisotropy in SAXS patterns. Interestingly enough, upon further increase in HA concentration, the SAXS anisotropy gradually disappears (last two rows in Figure 4). We may only speculate that this is the effect of the increased viscosity which prevents the alignment of DNA into any larger (ropelike) domains—there is simply not enough time for these to form during the sample flow.

Compression of DNA Subphase upon HA Addition. A feature more relevant to this work, visible in Figure 4, is the increase of the ring radius ($q^{\star}$) as C_{HA} increases. We illustrate this better using 1D SAXS pattern shown in Figure 5 for C_{DNA} = 10 g/L solution with an increasing HA content. Importantly, the increase in $q^{\star}$ with the increase in HA reflects the decrease

DOI: 10.1021/ma502090x
Macromolecules XXXX, XXX, XXX−XXX

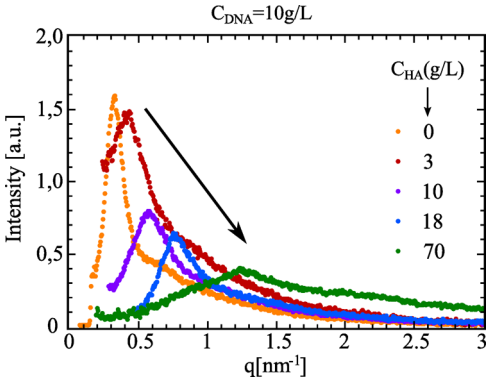

Figure 5. 1D-SAXS spectra of DNA/HA binary mixtures for C_{DNA} = 10 g/L with varying concentration of HA up to C_{HA} = 70 g/L. The increase in HA content shifts the scattering maximum $q^\star$ to higher values.

of the mean DNA interchain separation. In other words, the DNA subphase is compressed upon HA addition.

The evolution of $q^\star$ as a function of the monomer concentration ratio of the two PEs, c_{HA}/c_{DNA}, is presented in Figure 6. We have studied six different DNA initial

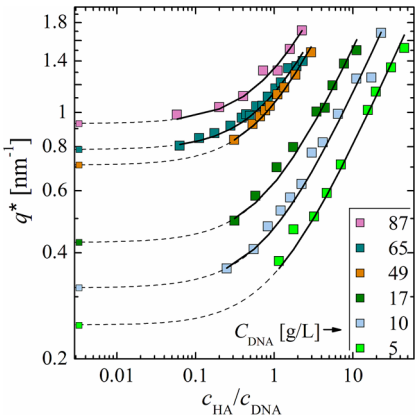

Figure 6. SAXS peak positions $q^\star$ shift up from the values for pure DNA mother solutions (points on the left *Y*-axis) upon addition of HA (shown as the increase in c_{HA}/c_{DNA}). For higher c_{HA}/c_{DNA} ratios the peaks shift according to a power law $q^\star \propto (c_{HA}/c_{DNA})^{1/2}$.

concentrations, and the results in Figure 6 show how the SAXS peaks shift upon addition of HA in comparison to HA-free DNA solutions (the points on the left axis). Our manner of presentation and the results shown in Figure 6 are qualitatively similar to those by Lai et al., who studied F-actin/DNA mixtures.[49] In that study, the primary scatterer is F-actin, the more rigid and more ordered mixture component, while DNA chains are the flexible, weakly scattering component that lacks ordering. The effective role of DNA chains is switched in DNA/HA mixture where now DNA is the more rigid, mesogenic, birefringent, and strongly scattering entity. For both systems, F-actin/DNA and DNA/HA here, $q^\star$ shifts up with an increase in the monomer concentration ratio of the two PEs, in our case even for very small amount of HA added, $c_{HA}/c_{DNA} \approx 0.1$. Lai et al. emphasize a power law dependence of $q^\star$ on the ratio $c_{DNA}/c_{F-actin}$. They find this for a rather narrow range of monomer concentration ratios from 1 to 6. In a similarly limited range of ratios, $1 < c_{HA}/c_{DNA} < 10$, we also find the same power law dependence. However, for the much lower c_{HA}/c_{DNA} ratios that we cover in our study, this dependence necessarily vanishes, as the $q^\star$ value approaches the $q_0^\star$ value for DNA alone (points on the *Y*-axis in Figure 6 and see also the Supporting Information Figure 1). Empirically, the $q^\star$ dependence is given by

$$q^\star = q_0^\star \sqrt{1 + \gamma c_{HA}/c_{DNA}} \quad (2)$$

as denoted with lines in Figure 6. The square-root dependence stems from the fact that $q^\star$ reflects the mesh size which scales with the square-root of the concentration (Supporting Information Figure 1). The factor γ will be further elaborated in the Discussion section, see eqs 6 and 7.

It is also noteworthy that the SAXS intensity ring is clear and relatively strong which indicates that, although in the DNA/HA solutions exist many separated DNA domains, all of them feature a similar characteristic length scale (see Supporting Information for the comparation of fwhm of the scattering peaks at each $q^\star$ presented in Figure 6 and fwhm of the scattering peaks for the DNA solutions without HA).

DISCUSSION

Complete Phase Separation? From the above we may conclude that we never observed a single phase HA/DNA mixture, for a rather broad range of mixture ratios (0.05−30) and total PE content 0.5−25%. That is, our SAXS data indicate that even the smallest amounts of HA added to the mixture were always to occupy a separate volume and reduce the volume available to DNA. This reflects the fact that the SAXS correlation peak of the mixture is always shifted upward in comparison to pure DNA (see Figure 6). These shifts can occur only if the DNA concentration increases upon HA addition. If HA completely intermixed with DNA and formed a single phase, then the latter would still occupy the same volume. In that case, the DNA concentration would not change—and the SAXS peak would not shift—contrary to our observation. Interestingly, mixing of the like charged (synthetic) polyelectrolytes and formation of a single phase has been found up to 5−15% of total PE content in water (i.e., 50−150 g/L[51]); from SAXS, our DNA/HA mixtures appear quite separated, even at 1% total PE content.

In accordance, polarizing microscopy (PLM) demonstrates the existence of separated phases, but it is not applicable in the low DNA/HA concentration range as 17 g/L (2% or lower) DNA solutions are not birefringent. Also, PLM does not inform on the possibility that some HA is mixed into DNA domains, and it is a plausible scenario that we need to investigate further. In the opposite case, DNA intermixed into HA domains would render these optically anisotropic, and we do observe the isotropic domains. Regardless, PLM is not quantitative and only provides qualitative information. In the following, we will analyze our data further by proposing a scenario where some HA mixes into DNA phase. As for the reasons just mentioned, as well as for simplicity, we do not consider the opposite—that some DNA mixes into the HA subphase.

We base the analysis on our experimental result that the SAXS peak originates from DNA subphase. In our recent paper,[52] we showed for DNA solutions across two decades in concentration from 2 to 200 g/L that—as expected in the framework of the scaling theory[2]—the relationship between $q^\star$ and concentration is precisely

$$q^\star = 2\pi(b_{DNA} n_{DNA})^{1/2} \quad (3)$$

DOI: 10.1021/ma502090x
Macromolecules XXXX, XXX, XXX−XXX

where b_{DNA} = 0.34 nm is the DNA monomer size and n_{DNA} is the monomer (basepair) number concentration (see also Supporting Information). Wang and Bloomfield[19] obtained before the same equation, although for the nucleosomal DNA 146bp fragments. For these, the studied concentration range was mainly below the liquid crystalline ordering concentration, unlike ours, which starts to show limited ordering amidst the studied range. Nevertheless, no shift is discernible in $q^\star$, or a change in slope away from 0.50 in our data within the experimental error. That is, the position of the scattering maximum $q^\star$ is a variable, which in the isotropic solution may be regarded as the measure of the characteristic length scale $\xi_{DNA} \propto 1/q^\star$ of an isotropic, random DNA mesh and upon alignment of DNA chains and precholesteric textures formation as an average distance $L_{DNA} \propto 1/q^\star$ between parallel chains. These two parameters are quite close in value and thus the $q^\star$ versus c dependence is unaffected by this qualitative change. One may read from eq 3 that the value of $q^\star$ is simply given by the total (contour) length of all DNA macroions constrained in a volume allocated to the DNA molecules. We found[52] that the equation holds for the weakly charged, however rather rigid HA, while Combet et al.[65] found that corrections are necessary for various flexible PEs.

Now, we start by assuming completely separated DNA and HA phases, and we denote coresponding volumes as $V^\star_{DNA}$ and $V^\star_{HA}$, where the total sample volume is $V = V^\star_{DNA}+V^\star_{HA}$. When we normalize to V we get $1 = V^\star_{DNA}/V + V^\star_{HA}/V$. This relationship may be expressed also with the effective concentrations of DNA and HA ($c^\star_{DNA}$, $c^\star_{HA}$, monomolar concentration) in those subphase volumes and by the nominal monomer concentrations c_{DNA} and c_{HA} (defined across the total volume - converted from the mass concentrations in Figure 1):

$$1 = c_{DNA}/c^\star_{DNA} + c_{HA}/c^\star_{HA} \quad (4)$$

Here we note that all the variables are experimentally accessible except $c^\star_{HA}$, thus:

$$c^\star_{HA} = c_{HA}/(1 - c_{DNA}/c^\star_{DNA}) \quad (5)$$

Using this expression and our SAXS length scale calibration expression ($((c^\star_{DNA})^{1/2}) \propto (2\pi/q^\star)$), we convert all the $q^\star$ data points for different DNA concentrations from Figure 6 to get the corresponding $c^\star_{DNA}$ values necessary for obtaining the $c^\star_{HA}$ value.

Interestingly, if we plot these data as $c^\star_{HA}$ versus $c^\star_{DNA}$ (see Figure 7), we get a simple linear relationship

$$c^\star_{HA} = \Gamma \times c^\star_{DNA} \quad (6)$$

where $\Gamma = 0.85 \pm 0.04$

The above result is directly related to the empirical relationship we presented before. That is, if we rewrite eq 4 by inserting eq 6, we get

$$c^\star_{DNA} = c_{DNA}\left(1 + \Gamma^{-1}\frac{c_{HA}}{c_{DNA}}\right) \quad (7)$$

which is analogous to eq 2, if we take into consideration that $q^\star \propto (c^\star_{DNA})^{1/2}$, $q^\star_0 \propto (c_{DNA})^{1/2}$ and $\gamma = \Gamma^{-1}$. If the effective concentration ratio from eq 6 is converted to a ratio of the characteristic length scales (mesh size) of two separated phases, DNA and HA, we obtain that $\xi_{HA} = 0.62\xi_{DNA}$. In other words, in the mixture, the HA mesh size is proportionally smaller than the DNA mesh size.

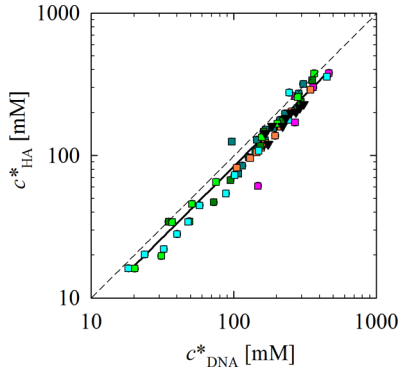

Figure 7. Effective concentration of HA versus the effective concentration of DNA is shown for the binary mixtures prepared by Protocol I (squares) and Protocol II (black triangles). The effective concentration of DNA is calculated from the experimentally obtained $q^\star$ measured for a given mixture (see Figure 1). The nominal concentrations of DNA and HA that define a mixture, as well as $c^\star_{DNA}$, enter the expression for calculation of $c^\star_{HA}$.

With the above relationships a (pseudo)ternary phase diagram (Figure 8a) may be constructed for the DNA/HA mixture, in analogy to the work on synthetic, like-charged PE mixtures by Hellebust et al.[51] The nominal concentrations of c_{DNA} and c_{HA} are the initial (gravimetrically determined)

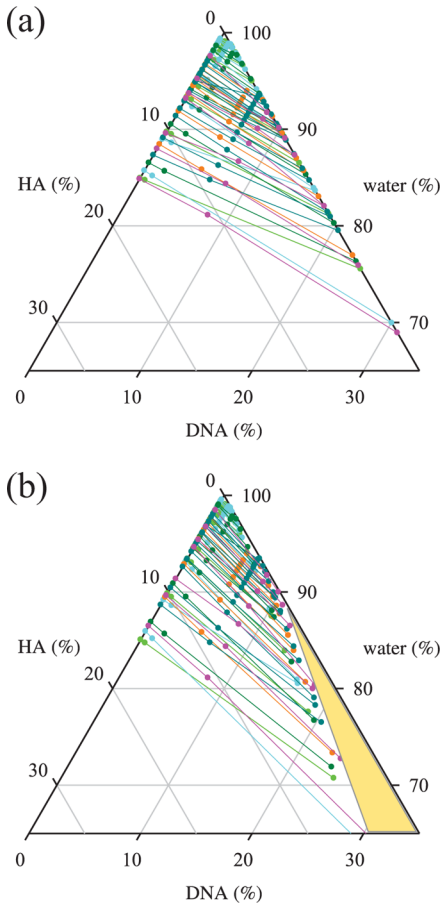

Figure 8. (a) Ternary phase diagram of DNA, HA, and water if no mixing is assumed. (b) Ternary phase diagram of DNA, HA, and water if mixing of HA into DNA is assumed. A single-phase region is denoted as a triangle.

DOI: 10.1021/ma502090x
Macromolecules XXXX, XXX, XXX−XXX

concentrations presented by midpoints of the tie-lines. The tie-lines connect the end points found at the edges of the triangular diagram. One end-point denotes the concentration of the DNA subphase (where HA is zero due to inmiscibility constraint) and the other of the HA subphase (where DNA is zero).

In accordance with our initial assumption, there is no mixing of the phases and there is no single phase region in the diagram.

Osmotic Pressure Equilibrium and Phase Separation. In the following and for the sake of completeness we question this assumption and suppose that a number fraction of HA molecules $\Delta \cdot N_H$ mixes into the DNA phase (for brevity, we will use indices H for HA and D for DNA.). We remind that $N_H/V = c_H$ and that $N_H/V_H^\star = c_H^\star$. Thus, the reduced concentration of pure HA phase, $c_{H\Delta}^\star$ would be

$$c_{H\Delta}^\star = c_H^\star \times (1 - \Delta) \tag{8}$$

Also, from the above follows that the concentration of mixed-in HA within the DNA subphase volume is $c_{H\Delta}^X = \Delta \cdot N_H/V_D^\star$. This can be written as $c_{H\Delta}^X = \Delta(N_H/V)(V/V_D^\star)$ which leads to

$$c_{H\Delta}^X = \Delta \times c_D^\star \times (c_H/c_D) \tag{9}$$

Notably, the concentration of mixed-in HA fraction depends on the ratio of nominal (initial) concentrations of HA and DNA— with more HA added, more mixing occurs. However, the Δ parameter still remains to be evaluated in order to define the phase diagram already presented in Figure 8b.

Toward this goal, we continue by reminding that DNA and HA subphases are in the osmotic equilibrium regulated mainly by counterions. That is, the osmotic pressure of the DNA subphase with a HA fraction mixed-in equals the pressure of the HA subphase:

$$\Pi_D^\star + \Pi_{H\Delta}^X = \Pi_{H\Delta}^\star \tag{10}$$

The osmotic pressure for DNA as a highly charged PE is defined by the osmotic pressure coefficient $\phi_D = (2\eta_D)^{-1}$ (η is the Manning parameter) and the counterion concentration $2c_D^\star$ (there are two counterions per monomer-basepair):

$$\Pi_D^\star \propto 2\phi_D \times c_D^\star \tag{11}$$

The osmotic pressure for HA as a weakly charged PE is defined by the osmotic pressure coefficient $\phi_H = 1-0.5\eta_H = 0.64$ ($\eta_H = 0.72$ for HA) and the counterion concentration $c_H^\star$.

We emphasize here that a conventional theoretical relationship between the pressure and free counterion concentration $\Pi/(RT) = \phi\, c$ is employed for this analysis. In the Introduction, we referred to the fact that for strong PEs like DNA or PSS the osmotic pressure scales as $\Pi/(RT) = \phi\, c^{9/8}$. Rigorously employing the exponent 9/8 would only complicate the analysis and the exposition here, whereas, quantitatively, the results would not differ as much. In other words, the coefficients that are considered here, Δ or Γ are of the order of 1, and whether they are exponentiated or not would only have minor effect on the quantities obtained, e.g., $0.5^{9/8} = 0.54$, but not on the general message. However, in the following section we will address the fact that the osmotic pressure of PEs actually follows the 9/8 scaling.

We now continue by equalizing the osmotic pressures of the two subphases, taking into account the possible intermixing, eq 9:

$$\phi_H c_{H\Delta}^\star = [2\phi_D + \Delta\phi_H \times (c_H/c_D)] \times c_D^\star \tag{12}$$

Then, we take into account the experimentally obtained relationship of effective concentrations of HA and DNA, eq 6, as well as eq 8 and get:

$$\Gamma\phi_H \times (1 - \Delta) = 2\phi_D + \Delta\phi_H \times (c_H/c_D) \tag{13}$$

This expression is the condition for intermixing of HA into DNA subphase. The expression may be satisfied for different values of parameters Δ, c_H/c_D and only for $\phi_D \leq 0.28$, that is

$$\Delta = (\Gamma - 2\phi_D/\phi_H)/(c_H/c_D + \Gamma) \tag{14}$$

If we take the Manning values of the osmotic coefficients for DNA, $\phi_D = 0.12$, and HA, $\phi_H = 0.64$, we get

$$\Delta = 0.47/(c_H/c_D + 0.85) \tag{15}$$

Thus, we obtain the fraction of HA within the DNA phase:

$$c_{H\Delta}^X/c_D^\star = 0.47 \times \frac{(c_H/c_D)}{c_H/c_D + 0.85} \tag{16}$$

Interestingly, the higher the relative HA content, the higher the fraction of HA which should mix into DNA. For the lowest HA contents that we tested, $c_H < 0.1 \times c_D$, the ratio of HA and DNA in DNA domains would be $0.47 \cdot (0.1/0.95) \sim 5\%$, while it would rise to 45% for the highest HA contents $c_H > 30 \times c_D$. That is, if we assume that there is some mixing of DNA and HA, the ternary phase diagram, Figure 8b, would feature a single phase mixture region. However, this region is broadening toward higher DNA or HA content, in contradiction with the case presented by Hellebust et al., where the single phase mixture occurs only at the lowest concentrations of PEs and disappears toward higher PE contents.[51] We find that such a feature that may be considered unphysical negates the initial assumption of mixing.

Osmotic Pressure Equilibrium and Manning Condensation Parameter. Importantly, unlike the osmotic pressure experiments by Essaffi et al. or Raspaud et al., we do not use an uncharged polymer as the stressing agent. We directly compare two PEs: DNA that features counterion condensation and HA that does not. However, being a PE, it still provides counterions into the solution. As there is no mixing of HA and DNA, the counterion concentrations achieve the Donnan equilibrium, as the osmotic pressures equalize between the DNA and HA subdomains. Our primary finding is that $\Pi_H^\star$ must obey the same scaling law as $\Pi_D^\star$, otherwise we could not observe the PE monomers concentrations to be proportional $\Gamma = c_H^\star/c_D^\star = 0.85$ across a broad concentration range 20−500 mM. We have already emphasized that the osmotic pressure scaling for strong PEs has been established to be $\Pi/(RT) \propto c^{9/8}$.[1,22,23] For a given monomer concentration $c_D^\star$ the counterion concentration for DNA is $2c_D^\star$ (two counterions and two phosphate groups per base pair) and for HA is $c_H^\star$ where we would also use $c_H^\star = 0.85c_D^\star$. The corresponding osmotic pressures are

$$\Pi_D^\star/RT \propto (2\phi_D c_D^\star)^{9/8} \tag{17}$$

$$\Pi_H^\star/RT \propto (0.85\phi_H c_D^\star)^{9/8} \tag{18}$$

and we arrive to a relationship of the osmotic coefficients

$$\phi_D = 0.42\phi_H \tag{19}$$

As there is no counterion condensation for HA we do not expect the concentration dependence of ϕ_H and settle for the

DOI: 10.1021/ma502090x
Macromolecules XXXX, XXX, XXX−XXX

theoretical value $\phi_H = 1-0.5\eta_H = 0.64$ based on the Katchalsky cell model.[11,13] Then we get $\phi_D = 0.28$, about double the Manning value $\phi_D = (2\eta)^{-1} = 0.12$ and close to what Raspaud et al. found for DNA $\phi_D = 0.24$.

The osmotic pressure coefficient for DNA, a strong polyelectrolyte, here comes as a concentration independent constant, while there is a large body of work where it is predicted that it should increase toward higher concentrations (for example, see refs 22−28). In these, the osmotic pressure is taken as $\Pi/(RT) \propto \phi(c)\cdot c$, while experimentally it is $\Pi/(RT) \propto \phi\, c^{9/8}$. We remind that if the pressure is normalized by c, then we will get $\Pi/(cRT) \propto \phi\, c^{1/8} \propto \phi(c)$. The 1/8 scaling amounts to an increase in $\phi(c)$ of 30% per order of magnitude in concentration. Indeed, in ref 23, we note an increase from $\phi(c) = 0.16$ to 0.21 for $c = 20-200$ mM concentration range; in ref 22, $\phi(c) = 0.20$ to 0.26 for the same range; in ref 25, $\phi(c) = 0.22$ to 0.35 across several orders of magnitude. Here we emphasize that because the 9/8 scaling is valid also for HA, where there is no counterion (de)condensation, then it is debatable whether the 1/8 component that defines $\phi(c)$ could be due to the (de)condensation.

As an illustration of the validity of the above considerations, in Figure 9 we present the literature osmotic pressure data for

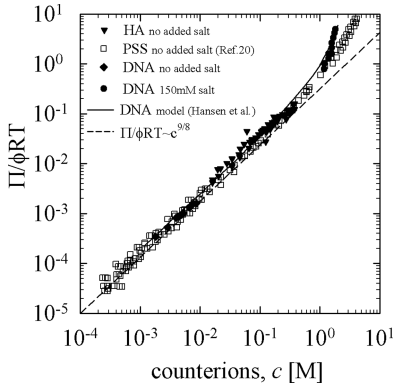

Figure 9. Equation of state for DNA, HA and PSS.[20] The osmotic pressure is rescaled by the osmotic coefficient of a given PE, where the osmotic coefficient for strong PEs (DNA, PSS) is η^{-1}, i.e., double the Manning theoretical value and for HA is $1-0.5\eta$[13] (η is the Manning parameter for a given PE).

DNA and PSS and compare it with our findings for HA. We plot on the x-axis the total counterion concentration c of the PEs in question and on the y-axis is the osmotic pressure rescaled by $RT\phi$ of the respective PE. The value of the osmotic coefficient for DNA has to be $\phi_D = 0.28$ in order for DNA and HA to fall on the single master curve. Importantly, if $\phi_P = 0.35$, double the Manning value, is used for normalizing PSS osmotic pressure data, we will arrive at a single (experimental) master curve for DNA, HA, and PSS. In other words, in the equation of state for all the PEs, there is the concentration-independent osmotic pressure coefficient: $\Pi/(RT) \propto \phi c^{9/8}$, where $\phi = \eta^{-1}$ for strong PEs or $\phi = 1-0.5\eta$ for the weak PEs.

SUMMARY

First, our study of a mixture of DNA and HA—a polyelectrolyte composite—is a novel combination of chain rigidity and charge density of polyion chains in the mixture. That is, HA is the flexible component here and it carries a weaker charge than DNA. However, it is not uncharged as PEG and it is quite closer in rigidity to DNA than DNA is to F-actin or to PEG.[1,49] In brief, F-actin/DNA, DNA/HA and DNA/PEG are three characteristic cases from a spectrum of possible DNA mixtures. In our case, HA and DNA components could be expected to phase separate either due to a difference in rigidity or due to being of the same charge.[35,66] The question is whether for HA and DNA the rigidity difference was sufficient, as there are works that indicated that mixing is possible for PEs of the same charge when the rigidity was matched.[50,51] By polarizing microscopy (PM), we have observed birefringent, microns thick, elongated domains. These appear already in mixtures with nominal DNA concentration of only 10 g/L, which is below the concentration for formation of anisotropic DNA phase. In coexistence were found optically isotropic domains of similar elongated shapes. HA solutions are not known to show birefringence at any concentration. That is, the phase separation elevated local, effective concetrations of DNA and HA in their domains and lead to ordering and birefringence in DNA. Eventually, we do attempt to quantitate the fraction of HA and DNA from the area of their respective domains, but this appears to be an imprecise method.

Second, from SAXS data, we managed to infer that the phase separation is complete and that there is no mixing-in of DNA into HA domains and vice versa. Others have shown[19] and we have checked that the DNA features a well-defined scattering maximum (polyelectrolyte peak) that depends on the square-root of the concentration. Importantly, this is a rather precise and reproducible feature (see Supporting Information). On the other hand, scattering from the HA system is significantly less intense and reveals, instead of a scattering maximum, only a weak shoulder but with a similar concentration dependence. What we established is that, also for the DNA/HA mixture the position of the scattering peak is a direct measure of local DNA concentration in the range of 2−200 g/L and beyond. This first provides the respective volumes taken by DNA or HA domains and eventually the effective HA concentration within those domains. Importantly, we find that the monomer concentrations of DNA and HA in the mixture are in a constant ratio across the concentration range studied.

Third, it is this precise knowledge of DNA and HA effective (local) concentrations that allowed us to infer osmotic pressure versus monomer concentration scaling to be the same $\Pi \propto c^{9/8}$ for HA as for DNA and other strong PEs, like PSS or actin.[1,20,49] That is, we infer this from the proportionality of concentrations of HA and DNA and from the necessary equilibrium of counterion-dominated osmotic pressures between the domains. Our result for HA complements the previously available results on osmotic pressure of HA in added salt environment.[43]

Most interestingly, since with HA there is no condensation, the osmotic coefficient ϕ is more clearly defined and the coefficient for HA may serve as a reference and let us evaluate the DNA coefficient. Our data corroborate the result by Raspaud et al.,[1] that for DNA in low salt conditions the osmotic coeficient may be double the theoretical one by Manning. Our comparison of data for DNA and another strong PE, PSS indicates that this doubling is a common feature.

In brief, the osmotic pressure of PEs, strong or weak, with or without counterion condensation scales as $\Pi \propto c^{9/8}$. This should be taken into account when proposing that the osmotic coefficient ϕ for strong PEs is concentration dependent due to counterion decondensation being enhanced at higher concentrations. We point out that the concentration dependence

DOI: 10.1021/ma502090x
Macromolecules XXXX, XXX, XXX−XXX

ascribed to decondensation might simply be due to a $c^{1/8} \propto \Pi/c \propto c^{9/8}/c$ factor. The deviation from $\Pi \propto c$ appears already in simple scaling relationships for PEs, where only the Manning's concentration-independent counterion condensation is taken into account.

■ ASSOCIATED CONTENT

Supporting Information

We provide the calibration relationship of the mesh size correlation length obtained by SAXS versus DNA concentration. We also provide the evidence that the SAXS scattering peak for a given DNA concentration is not broadened by the presence of HA subdomains. Finally, we present an analysis of PLM images where the contents of birefringent (i.e., DNA) and nonbirefringent (i.e., HA phase) is quantitated. This material is available free of charge via the Internet at http://pubs.acs.org.

■ AUTHOR INFORMATION

Corresponding Author

*E-mail: tvuletic@ifs.hr. Phone: +385 14 69 88 87. Fax: +385 14 69 88 89.

Notes

The authors declare no competing financial interest.

■ ACKNOWLEDGMENTS

We gratefully acknowledge Elettra-Sincrotrone, Trieste for the beam-time. This work is primarily based on the support from the Unity through Knowledge Fund, Croatia under Grant 17/13 "Confined DNA" and also Grant 22/08. D. Grgičin and K. Salamon were also supported by the Croatian Ministry of Science, Education and Sports under grants 035-0000000-2836 and 035-0352843-2844.

■ REFERENCES

(1) Raspaud, E.; da Conceiçao, M.; Livolant, F. *Phys. Rev. Lett.* **2000**, *84*, 2533−2536.
(2) de Gennes, P.-G.; Pincus, P.; Velasco, R. M.; Brochard, F. *J. Phys. (Paris)* **1976**, *37*, 1461.
(3) Rubinstein, M.; Colby, R. H. *Polymer Physics*; Oxford University Press: Oxford, U.K., 2003.
(4) van der Maarel, J. R. C. *Introduction to Biopolymer Physics*; World Scientific: Singapore, 2007.
(5) Dobrynin, A. V.; Rubinstein, M. *Prog. Polym. Sci.* **2005**, *30*, 1049−1118.
(6) Odijk, T. *J.Polym. Sci. Polym. Phys. Ed.* **1977**, *15*, 477−483.
(7) Skolnick, J.; Fixman, M. *Macromolecules* **1977**, *10*, 944−948.
(8) Odijk, T. *Macromolecules* **1979**, *12*, 688−693.
(9) Baumann, C. G.; Smith, S. B.; Bloomfield, V. A.; Bustamante, C. *Proc. Natl. Acad. Sci. U.S.A.* **1997**, *94*, 6185−6190.
(10) Ullner, M. *J. Phys. Chem. B* **2003**, *107*, 8097−8110.
(11) Lifson, S.; Katchalsky, A. *J. Polym. Sci.* **1954**, *13*, 43−55.
(12) Oosawa, F. *Polyelectrolytes*; Marcel Dekker: New York, 2007; Chapter 5.
(13) Manning, G. S. *J. Chem. Phys.* **1969**, *51*, 924−933.
(14) Förster, S.; Schmidt, M. *Adv. Polym. Sci.* **1995**, *120*, 51−133.
(15) Netz, R. R.; Andelman, D. *Phys. Rep.* **2003**, *380*, 1−95.
(16) Andresen, K.; Qiu, X.; Pabit, S. A.; Lamb, J. S.; Park, H. Y.; Kwok, L. W.; Pollack, L. *Biophys. J.* **2008**, *95*, 287−295.
(17) Wong, G. C.; Pollack, L. *Annu. Rev. Phys. Chem.* **2010**, *61*, 171−189.
(18) Mazur, A. K.; Maaloum, M. *Phys. Rev. Lett.* **2014**, *112*, 0681041−0681045.
(19) Wang, L.; Bloomfield, V. A. *Macromolecules* **1991**, *24*, 5791−5795.
(20) Wang, L.; Bloomfield, V. A. *Macromolecules* **1990**, *23*, 804−809.
(21) Auer, H. E.; Alexandrowicz, Z. *Biopolymers* **1969**, *8*, 1−20.
(22) Hansen, P. L.; Podgornik, R.; Parsegian, V. A. *Phys. Rev. E* **2001**, *64*, 0219071.
(23) Essafi, W.; Lafuma, F.; Baigl, D.; Williams, C. E. *Eur.Phys.Lett.* **2005**, *71*, 938−946.
(24) Nyquist, R. M.; Ha, B.-Y.; Liu, A. J. *Macromolecules* **1999**, *32*, 3481−87.
(25) Antypov, D.; Holm, C. *Phys. Rev. Lett.* **2006**, *96*, 0883021−4.
(26) Deshkovski, A.; Obukhov, S.; Rubinstein, M. *Phys. Rev. Lett.* **2001**, *86*, 2341.
(27) Donley, J. P.; Heine, D. R.; Wu, D. T. *Macromolecules* **2005**, *38*, 1007−1020.
(28) Liao, Qi.; Dobrynin, A. V.; Rubinstein, M. *Macromolecules* **2003**, *36*, 3399−3410.
(29) Lerman, L. S. *Proc. Natl. Acad. Sci. U.S.A.* **1971**, *68*, 1886−1890.
(30) Vasilevskaya, V. V.; Khokhlov, A. R.; Matsuzawa, Y.; Yoshikawa, K. *J. Chem. Phys.* **1995**, *102*, 6595−6602.
(31) Maniatis, T.; Venable, J. H.; Lerman, L. S. *J. Mol. Biol.* **1974**, *84*, 37−64.
(32) Rau, D. C.; Lee, B. K.; Parsegian, V. A. *Proc. Natl. Acad. Sci. U.S.A.* **1984**, *81*, 2621−2625.
(33) Podgornik, R.; Rau, D. C.; Parsegian, V. A. *Macromolecules* **1989**, *22*, 1780−1786.
(34) de Vries, R. *Biophys. J.* **2001**, *80*, 1186−1194.
(35) Khokhlov, A. R.; Nyrkova, I. A. *Macromolecules* **1992**, *25*, 1493−1502.
(36) Buhler, E.; Boue, F. *Macromolecules* **2004**, *37*, 1600−1610.
(37) Lee, G. M.; Johnstone, B.; Jacobson, K.; Caterson, B. J. *Cell. Biol.* **1993**, *123*, 899−907. The dynamic structure of the pericellular matrix on living cells
(38) Evanko, S. P.; Tammi, M. I.; Tammi, R. H.; Wight, T. N. *Adv. Drug Delivery Rev.* **2007**, *59*, 1351−65.
(39) Horkay, F. *J. Polym. Sci. B Polym. Phys.* **2012**, *50*, 1699−1705.
(40) *Essentials of Glycobiology*, 2nd ed.; Varki, A., Cummings, R. D., Esko, J. D., Freeze, H. H., Stanley, P., Bertozzi, C. R., Hart, G. W., Etzler, M. E., Eds.; Cold Spring Harbor Laboratory Press: Cold Spring Harbor, NY, 2009.
(41) Horkay, F.; Hecht, A.-M.; Geissler, E. *J. Polym. Sci., Part B: Polym. Phys.* **2006**, *44*, 3679−3686.
(42) Horkay, F.; Hecht, A.-M.; Rochas, C.; Basser, P. J.; Geissler, E. *J. Chem. Phys.* **2006**, *125*, 2349041.
(43) Horkay, F.; Basser, P. J.; Londono, D. J.; Hecht, A.-M.; Geissler, E. *J. Chem. Phys.* **2009**, *131*, 1849021.
(44) Cleland, R. L. *Arch. Biochem. Biophys.* **1977**, *180*, 57−68.
(45) Ribitsch, G.; Schurz, J.; Ribitsch, V. *Colloid Polym. Sci.* **1980**, *258*, 1322−1334.
(46) Cowman, M. K.; Matsuoka, S. *Carbohydr. Res.* **2005**, *340*, 791−809.
(47) Whistler, R. L.; Olson, E. J. *Adv. Carbohydr. Chem.* **1957**, *12*, 299−319.
(48) Villetti, M.; Borsali, R.; Diat, O.; Soldi, V.; Fukada, K. *Macromolecules* **2000**, *33*, 9418.
(49) Lai, G. H.; Butler, J. C.; Zribi, O. V.; Smalyukh, I. I.; Angelini, T. E.; Purdy, K. R.; Golestanian, R.; Wong, G. C. L. *Phys. Rev. Lett.* **2008**, *101*, 2183031−4.
(50) Piculell, L.; Nilsson, S.; Falck, L.; Tjerneld, F. *Polymer comm.* **1991**, *32*, 158−160.
(51) Hellebust, S.; Nilsson, S.; Blokhus, A. M. *Macromolecules* **2003**, *36*, 5372−5382.
(52) Salamon, K.; Aumiler, D.; Pabst, G.; Vuletić, T. *Macromolecules* **2013**, *46*, 1107−1118.
(53) Tomić, S.; Vuletić, T.; Dolanski Babić, S.; Krča, S.; Ivanković, D.; Griparić, L.; Podgornik, R. *Phys. Rev. Lett.* **2006**, *97*, 0983031−4.
(54) Tomić, S.; Dolanski Babić, S.; Vuletić, T.; Krča, S.; Ivanković, D.; Griparić, L.; Podgornik, R. *Phys. Rev. E* **2007**, *75*, 0219051−13.
(55) Vuletić, T.; Dolanski Babić, S.; Ivek, T.; Grgičin, D.; Tomić, S.; Podgornik, R. *Phys. Rev. E* **2010**, *82*, 0119221.
(56) Tomić, S.; Dolanski Babić, S.; Ivek, T.; Vuletić, T.; Krča, S.; Livolant, F.; Podgornik, R. *Europhys. Lett.* **2008**, *81*, 680031.

DOI: 10.1021/ma502090x
Macromolecules XXXX, XXX, XXX−XXX

(57) Kaji, K.; Urakawa, H.; Kanaya, T.; Kitamaru, R. *J. Phys. (France)* **1988**, *49*, 993−1000.
(58) Ito, K.; Yagi, A.; Ookubo, N.; Hayakawa, R. *Macromolecules* **1990**, *23*, 857−862.
(59) Amenitsch, H.; Rappolt, M.; Kriechbaum, M.; Mio, H.; Laggner, P.; Bernstorff, S. *J. Synchrotron Radiat.* **1998**, *5*, 506−508.
(60) Livolant, F.; Leforestier, A. *Prog. Polym. Sci.* **1996**, *21*, 1115−1164.
(61) Merchant, K.; Rill, R. L. *Macromolecules* **1994**, *27*, 2365−2370.
(62) Merchant, K.; Rill, R. L. *Biophys. J.* **1997**, *73*, 3154−3163.
(63) Livolant, F. *J. Phys. (Paris)* **1987**, *48*, 1051−1066.
(64) Wang, Z.-G.; Xia, Z.-Y.; Yu, Z.-Q.; Chen, E.-Q.; Sue, H.-J.; Han, C. C.; Hsiao, B. S. *Macromolecules* **2006**, *39*, 2930−2939.
(65) Combet, J.; Isel, F.; Raviso, M.; Boue, F. *Macromolecules* **2005**, *38*, 7456−7469.
(66) Flory, P. J. *Macromolecules* **1978**, *11*, 1138−1141.

DOI: 10.1021/ma502090x
Macromolecules XXXX, XXX, XXX−XXX